A EUROPEAN JOURNAL

CHEMPHYSCHEM

OF CHEMICAL PHYSICS AND PHYSICAL CHEMISTRY

Accepted Article

Title: Quantitative Comparison of Enzyme Immobilization Strategies for Glucose Biosensing in Real-Time Using Fast-Scan Cyclic Voltammetry Coupled with Carbon-Fiber Microelectrodes

Authors: Samantha K Smith, Leyda Z. Lugo-Morales, Christina Tang, Saahj P. Gosrani, Christie A. Lee, James G. Roberts, Stephen W. Morton, Gregory S. McCarty, Saad A. Khan, and Leslie A. Sombers

To be cited as: *ChemPhysChem* 10.1002/cphc.201701235

Link to VoR: http://dx.doi.org/10.1002/cphc.201701235

A Journal of ChemPubSoc Europe

WILEY-VCH

www.chemphyschem.org

10.1002/cphc.201701235

Quantitative Comparison of Enzyme Immobilization Strategies for Glucose Biosensing in Real-Time Using Fast-Scan Cyclic Voltammetry Coupled with Carbon-Fiber Microelectrodes

S.K. Smith[a], L.Z. Lugo-Morales[a], C. Tang[b], S.P. Gosrani[a], C.A. Lee[a], J.G. Roberts[a], S.W. Morton[a, b], G.S. McCarty[a], S.A. Khan[b], and L.A. Sombers*[a]

Abstract

Electrochemical monitoring of non-electroactive species requires a biosensor that is stable and selective, with sensitivity to physiological concentrations of targeted analytes. We have combined glucose oxidase-modified carbon-fiber microelectrodes with fast-scan cyclic voltammetry for real-time measurements of glucose fluctuations in brain tissue. Work presented herein quantitatively compares three approaches to enzyme immobilization on the microelectrode surface - physical adsorption, hydrogel entrapment, and entrapment in electrospun nanofibers. The data suggest that each of these methods can be used to create functional microbiosensors. Immobilization of glucose oxidase by physical adsorption generates a biosensor with poor sensitivity to glucose and unstable performance. Entrapment of glucose oxidase in poly(vinyl alcohol) nanofibers generates microbiosensors that are effective for glucose measurements over a large linear range, and that may be particularly useful when targeting glucose concentrations in excess of 3 mM, such as in blood. Hydrogel entrapment is the most effective in terms of sensitivity and stability. These microbiosensors can be used for simultaneous monitoring of glucose and dopamine in real time. The findings outlined herein should be applicable to other oxidase enzymes, and thus they are broadly important for the development of new tools for real-time measurements of fluctuating molecules that are not inherently electroactive.

[a] Department of Chemistry
NC State University
2620 Yarbrough Dr., Campus Box 8204
Raleigh, NC. 27695-8204

[b] Department of Chemical and Biomolecular Engineering
NC State University
Centennial Campus
911 Partners Way, Campus Box 7905
Raleigh, NC. 27695-7905

Introduction

Since the development of the glucose electrode in 1962 by Clark and Lyons,[1] biosensors have been implemented in various fields of study including the food industry, environmental monitoring, and in clinical applications.[2] Importantly, biosensors enable non-electroactive molecules, such as glucose, to be monitored with standard electrochemical methods. For example, glutamate, [3, 4] acetylcholine,[5, 6] lactate,[7] and glucose,[8-10] can be monitored via the generation of the electroactive mediator, hydrogen peroxide (H_2O_2). In the development of stable, sensitive, and reliable biosensors, the enzyme immobilization step is a crucial.[11] As such, the biosensing field has continually explored enzyme immobilization conditions to optimize specificity, stability, and biosensor response time. [12, 13]

Amperometry is the electroanalytical detection scheme that is most commonly coupled with enzyme-based sensors for neurochemical monitoring.[11] With this approach, a constant potential is applied to the electrode to drive redox processes that can be monitored with sub-millisecond temporal resolution. The measured current is directly proportional to the amount of species electrolyzed. However, all electroactive species that oxidize or reduce at the fixed potential add to the faradaic current, requiring additional strategies to limit the contribution from interfering analytes. These strategies often introduce limitations, such as slow response times due to the incorporation of chemically selective coatings, or spatial averaging across recording sites.[14] This has led to the investigation of other methods for *in situ* monitoring that enable real-time measurements with high spatiotemporal resolution, as well as selectivity.

Background-subtracted fast-scan cyclic voltammetry (FSCV) has recently emerged as an advantageous alternative for electroanalytical biosensing.[8, 9, 15] This technique is most often coupled with carbon-fiber microelectrodes and used for selective quantification of fluctuating

electroactive neurotransmitters, such as dopamine, in live brain tissue.[16-19] It offers a combination of selectivity, sensitivity, and temporal resolution that has enabled unprecedented insight into biological processes that range from release and re-uptake kinetics[20] to specific behavioral manifestations in awake subjects[17-19, 21]. Carbon-fiber microelectrodes are not as commonly used for biosensing as Pt electrodes; however, they offer several important advantages for electrochemical measurements in complex biological environments[22]. The small size allows for minimal tissue damage and measurements in discrete regions of the brain.[23, 24] The carbon is nontoxic, resists biofouling, and is commercially available at a low cost. It boasts a wide potential window in aqueous solutions,[25, 26] and the presence of oxygen-containing functional groups on the carbon surface facilitates electron transfer.[27-29] These carbon electrodes can be modified with glucose oxidase (GOx) to monitor glucose fluctuations in live brain tissue with sub-second temporal resolution.[8, 9] We have used this tool to simultaneously measure glucose and dopamine fluctuations at single recording sites in the rat striatum, directly demonstrating that glucose fluctuations are coupled with metabolic demand.[9]

In the present work, we quantitatively compare three GOx immobilization strategies for the detection of glucose at carbon-fiber microelectrodes coupled with FSCV. Specifically, we assess the sensitivity and stability of glucose detection when the enzyme is physically adsorbed onto the electrode surface and subsequently stabilized by a Nafion membrane, or when it is immobilized using entrapment in electrospun nanofibers or in a chitosan hydrogel, as previously established.[8, 9] The results demonstrate that entrapment of GOx in the chitosan hydrogel is most effective, in terms of sensitivity and stability, for monitoring physiological

brain glucose concentrations in the rat brain. However, entrapment in electrospun nanofibers is advantageous for monitoring glucose at higher concentrations (> 3 mM). Importantly, the immobilization strategies characterized herein can be adapted to other enzymes, to expand the development of tools targeting a variety of non-electroactive target molecules.

Results and Discussion

Three strategies for the immobilization of GOx on the surface of carbon-fiber microelectrodes were investigated; these are physical adsorption, hydrogel entrapment and entrapment in electrospun nanofibers. Figure 1 depicts a schematic overview of the fabrication procedure for each approach. Representative scanning electron micrographs (SEMs) of the finished GOx enzyme-modified electrodes are also included (scale bar 50 µm). Differences are easily observed at higher magnifications (inset images; scale bar 10 µm). For comparison, bare carbon-fiber microelectrodes exhibit clear and distinct vertical striations, as shown in Figure 2A. The white arrow highlights the transition from the glass insulation to the active carbon surface.

10.1002/cphc.201701235

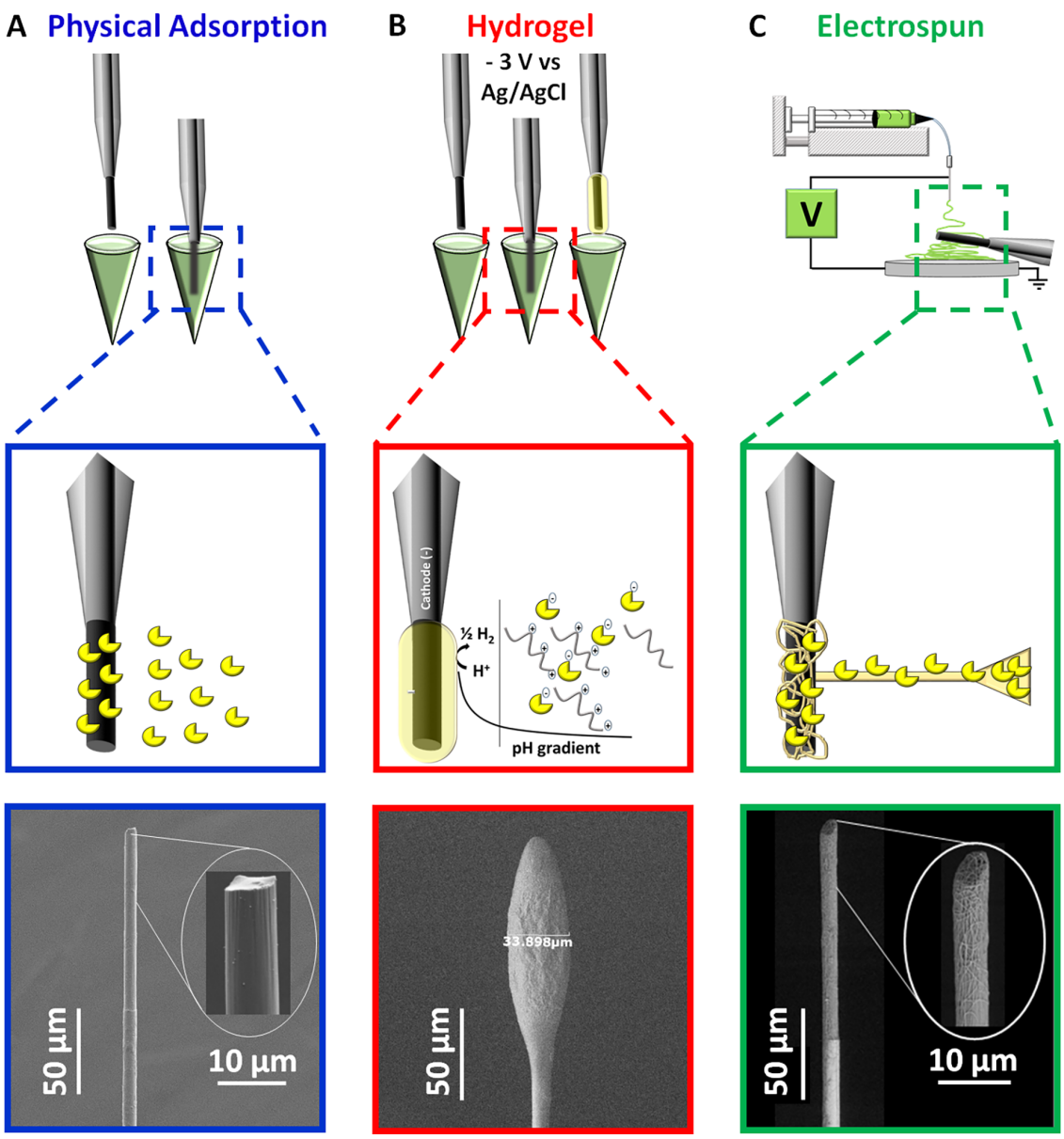

Figure 1. GOx immobilization strategies. (A) Immobilization via physical adsorption. Electrochemically pre-conditioned carbon-fiber microelectrodes are placed in GOx solution for 72 hours at 4°C. Bottom: representative scanning electron micrographs. (B) A chitosan hydrogel is created by applying a potential sufficient to reduce hydrogen in a 2% chitosan GOx solution. The representative SEM (bottom) depicts the membrane coating and a prolate spheroid electrode geometry. (c) Immobization in electrospun nanofibers is achieved by dispensing a

PVA GOx solution through a syringe (0.5 $ml \cdot hr^{-1}$) with a 17.5 kV potential applied and manual rotation of the electrode to ensure an even coating.

Physical adsorption of GOx is fundamentally the most straightforward strategy evaluated. This approach leverages weak Van der Waal's forces and electrostatic and/or hydrophobic interactions to immobilize the enzyme to the carbon sensing surface.[2] This immobilization strategy has been widely utilized due to its simplicity, including at carbon-fiber microelectrodes.[30] It is generally non-destructive to the enzyme, and boasts reduced production costs as compared to other immobilization methods.[31, 32] Carbon-fiber microelectrodes were electrochemically pre-conditioned by applying a triangular voltammetric waveform (−0.4 V to +1.4 V) for approximately 15 min at a frequency of 60 Hz, and then ~ 5 min at 10 Hz. Conditioned electrodes were soaked for 72 h in GOx solution at 4°C (Figure 1A; see Methods for details). Although this adsorption approach can theoretically work alone, our initial results were inconsistent (data not shown). Therefore, a Nafion film was adsorbed onto the enzyme-modified sensor to improve stability.[33, 34] Figure 1A depicts a scanning electron micrograph (SEM) of the finished electrode. The surface appears smooth, albeit with an uneven coating of material (inset).

The hydrogel entrapment strategy employs electrochemistry to control the solubility of chitosan, a low cost and nontoxic, natural polyaminosaccharide.[35, 36] Entrapment of GOx in a chitosan hydrogel immobilizes the enzyme at the pre-conditioned carbon surface without covalently binding the enzyme, as this has been shown to adversely impact enzyme activity.[2] The immobilization strategy has been described previously,[8, 9] and is depicted in Figure 1B.

Briefly, the conditioned electrode is submerged in mildly acidic chitosan solution (pH < 6.5) that contains GOx. Chitosan solubility is electrochemically controlled by the application of a negative potential sufficient to reduce hydrogen ions to hydrogen gas. In doing so, a steep pH gradient is generated immediately adjacent to the electrode surface. This initiates polymerization of the chitosan, affording entrapment of the GOx at the sensing surface. As demonstrated previously,[8] the hydrogel immobilization strategy creates a prolated spheroid or cotton swab-like electrode geometry (Figure 1B SEM).

Finally, electrospun poly(vinyl alcohol) (PVA) nanofibers were used to trap GOx at the carbon-fiber microelectrode surface. Electrospun nanofibers offer many advantages, including a high specific surface area[13, 37] that enables effective mass transfer to the electrode surface, which is critical to achieve optimized biosensor response times.[13, 38] PVA is a hydrophilic and biocompatible polymer that boasts excellent chemical and thermal stability.[39, 40] Enzyme immobilization is achieved by dispensing a PVA and GOx blend through a syringe (0.5 $ml \cdot hr^{-1}$) with a 17.5 kV potential applied (Figure 1C). This produces ejection of a polymer solution from the syringe needle aimed at a collector plate. As the electric field increases, the droplet takes a conical shape known as a Taylor cone, and a liquid jet forms from the tip of the cone. The fluid is converted into a solid fiber as the electrified jet is continuously stretched, due to repulsions between surface charges and the evaporation of solvent. [39, 41] The electrode is manually rotated in the electric field during electrospinning. Finally, hydroxyl groups on the PVA nanofibers (and the immobilized GOx itself) are crosslinked via glutaraldehyde vapor in an acidic environment.[39] This renders the nanofibers insoluble in water, improves stability, and increases mechanical strength.[42, 43] Figure 1C includes a representative SEM of a completed,

electrospun enzyme-modified carbon-fiber microelectrode, demonstrating randomly oriented, insoluble PVA nanofibers on the surface.

Fast-Scan Cyclic Voltammetry.

Background-subtracted fast-scan cyclic voltammetry (FSCV) can be employed to quantitatively characterize the performance of these microbiosensors. H_2O_2 is readily detected with this approach using a bare carbon-fiber microelectrode,[30] and this can be leveraged at microbiosensors to detect enzymatically-generated H_2O_2, and to thus report on rapid changes in glucose concentration.[8, 9] For the detection of H_2O_2, a triangular potential waveform (+0.1V to +1.4 V) is applied to a carbon-fiber microelectrode at a frequency of 10 Hz, using a scan rate of 400 $V \cdot s^{-1}$ (Figure 2A). During the application of potential, the current generated at the electrode surface is recorded. Representative recordings in the presence and absence of H_2O_2 are shown in Figure 2A (bottom left). To facilitate visualization of changes in the concentration of H_2O_2 at the electrode surface, a 'background' cyclic voltammogram collected prior to infusion of H_2O_2 is subtracted from subsequent voltammograms collected in the presence of H_2O_2 to generate background-subtracted voltammograms (Figure 2A, bottom right). These can be used to identify H_2O_2 by way of the single, well-defined oxidation peak near the switching potential (+1.4 V). Fluctuations in H_2O_2 concentration can be visualized over time using a color plot (Figure 2B, left), which provides an easy way to visualize and interpret the data. The x-axis contains information on collection time, the y-axis depicts the applied potential, and the z-axis (color) depicts the collected current. The magnitude of the H_2O_2 oxidation peak is correlated to concentration by way of standard calibration.

10.1002/cphc.201701235

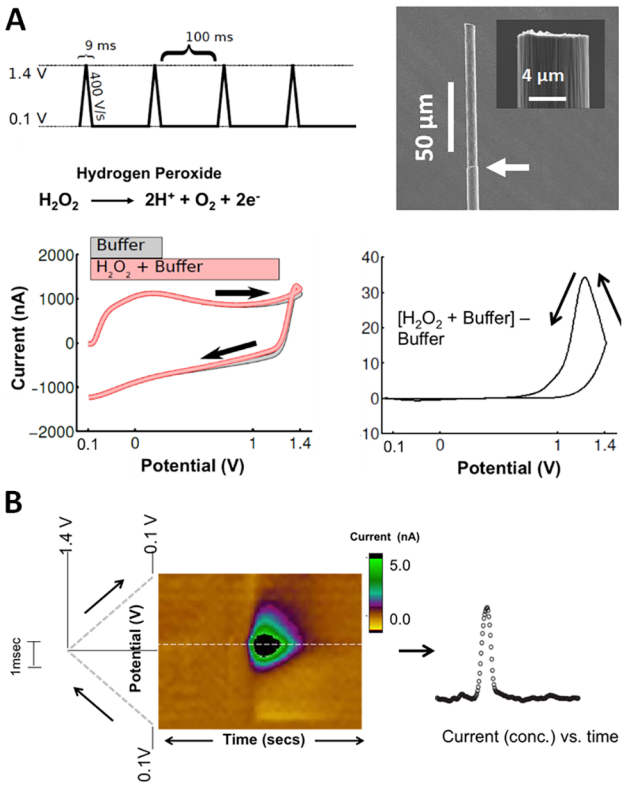

Figure 2. Fast-scan cyclic voltammetry for detection of H_2O_2. (A) A triangular waveform is applied with a scan rate of 400 $V \cdot s^{-1}$ (top left). A large background current is generated (bottom left, gray). Additional faradaic current is generated at a bare carbon-fiber microelectrode (top right) in the presence of H_2O_2 (pink). Subtraction of these signals generates a background-subtracted cyclic voltammogram (CV), which serves to identify and quantify H_2O_2 (bottom right). (B) Sequentially collected CVs are plotted with time (sec) on the x-axis, potential (V) on the y-axis, and current (nA) in color.

Figure 3A contains representative voltammetric data collected for each of the electrode immobilization strategies in a benchtop flow-injection apparatus before and after a 2 sec bolus injection of glucose (1.6 mM). Note that differences in sensitivity to glucose necessitate the use

10.1002/cphc.201701235

of different current scales on these color plots. This is easily visualized in Figure 3B, which provides current (nA) vs time (sec) traces extracted from the corresponding color plots in Figure 3A. It is clear that microbiosensors fabricated using the physical adsorption method (blue) were less responsive to glucose than those fabricated using the chitosan hydrogel (red) or the electrospun nanofiber (green) entrapment strategies.

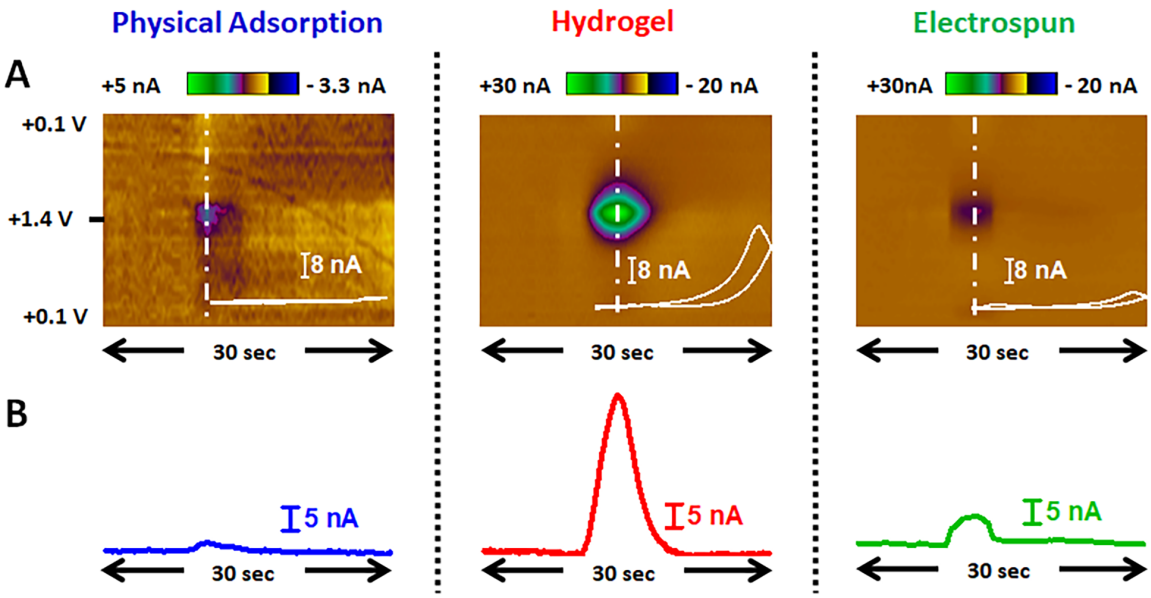

Figure 3. Glucose monitoring with FSCV at carbon microbiosensors created using physical adsorption of GOx (blue), hydrogel entrapment (red), and entrapment in electrospun nanofibers (green). (A) 30 sec of representative data demonstrating biosensor response to a 2 sec bolus of glucose (1.6 mM). Analyte identification is achieved by extracting voltammograms (inset) at the time indicated by the white dashed line. (B) Current vs time profiles extracted from the corresponding color plots shown in (A).

Sensitivity and Stability.

10.1002/cphc.201701235

In order to quantitatively evaluate sensitivity to glucose, the sensors were calibrated *in vitro* using the flow-injection apparatus described above. After electrochemical conditioning (described in Methods), glucose calibration curves were constructed. Sensitivity to glucose is reported as mean ± standard error of the mean (SEM) (Figure 4 and Table 1). The sensitivity to glucose encompasses a large range (~0.4 – 15 nA·mM^{-1} glucose). Analysis with one-way ANOVA reveals significant differences between the three enzyme immobilization strategies ($F(2,8) = 719$, ****$p<0.0001$), with the highest sensitivity achieved using the chitosan hydrogel entrapment approach (Figure 4A,B). The extended calibration curve (Figure 4A) reveals that chitosan-immobilized enzyme activity was saturated at glucose concentrations greater than ~3 mM. However, these microbiosensors demonstrated a linear response to glucose over a physiological range of brain glucose concentrations (< 3 mM).[14, 44] Enzyme entrapment using electrospun nanofibers resulted in microbiosensors that were less sensitive to glucose when compared to the chitosan hydrogel probes; however, it is notable that this strategy is effective for the detection of an increased range of glucose concentrations (0.2 - 50 mM). Although not sufficiently sensitive for typical, physiological concentrations of brain glucose, this approach may be suited for detection of elevated brain glucose concentrations under pathophysiological conditions, in glucose monitoring applications in the periphery (blood), or in the food industry. Indeed, increased glucose concentrations have been reported in the peripheral nervous system (3.9 - 7.8 mM, adult rats).[45]

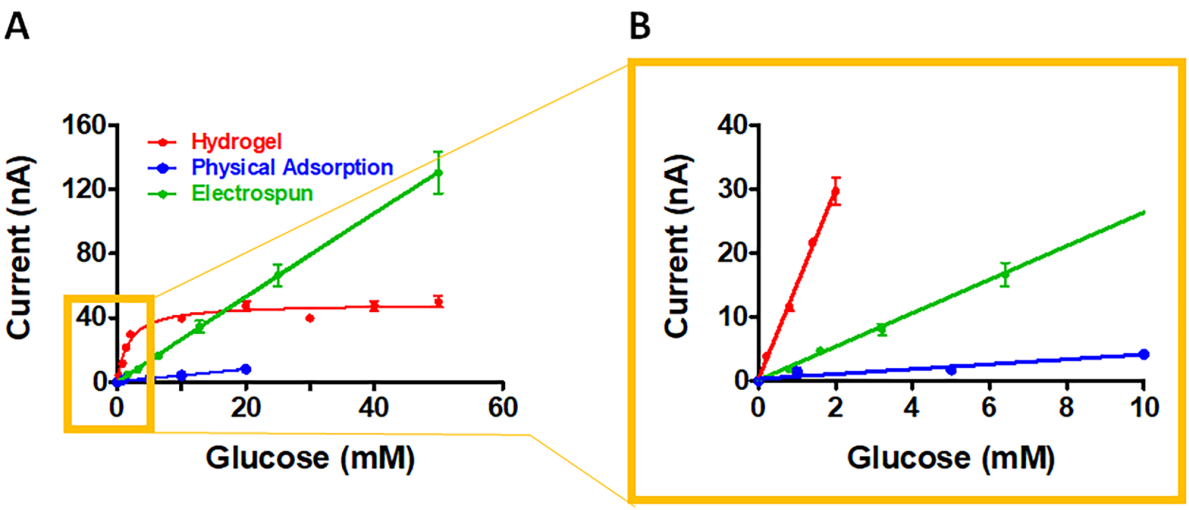

	Physical Adsorption	Hydrogel	Electrospun
Sensitivity (nA/mM)	0.38 ± 0.03	14.8 ± 0.3	2.62 ± 0.01
% Difference from Hydrogel	~ - 97.4%	0.0 %	~ -82.3 %

Figure 4. Sensitivity to glucose. (A) Calibration plots (0.2-50 mM), (B) Expanded view of more physiologically appropriate concentrations for glucose measurements in brain. (C) Sensitivities reported in terms of percent difference from the established hydrogel entrapment strategy for enzyme immobilization.

Microbiosensor stability was assessed over a 4 h period (Figure 5A), as this is approximately the length of a typical in vivo FSCV experiment. 2-sec bolus injections of glucose were delivered to the biosensor surface every 15 min (the linear-range median concentration for each immobilization strategy was selected). Normalized signals (mean ± SEM) were evaluated to

assess biosensor stability across time. The color plots (Figure 5B) depict representative data collected with each of the three enzyme immobilization strategies investigated. Data are shown for the first (top) and last (bottom) glucose samples investigated over the recording session. Two-way ANOVA reveals significant differences between microbiosensors fabricated with the various immobilization strategies ($F(2, 119) = 237.9$, $^{***}p<0.001$). GOx immobilization by way of physical adsorption generates biosensors that are not stable, as ~ 42% of current is lost after the first injection (blue). Indeed, all responsivity to glucose is lost in the first 30 min of experimentation potentially due to the weak interactions between the enzyme and carbon surface. Microbiosensors fabricated with GOx immobilized in electrospun nanofibers are relatively stable, but they exhibit a ~ 75% decline in response relative to the first injection after 2.75 h of measurements (green). Finally, the chitosan hydrogel enzyme immobilization strategy generates a stable response across all time points (red), consistent with previously published results.[8, 9]

10.1002/cphc.201701235

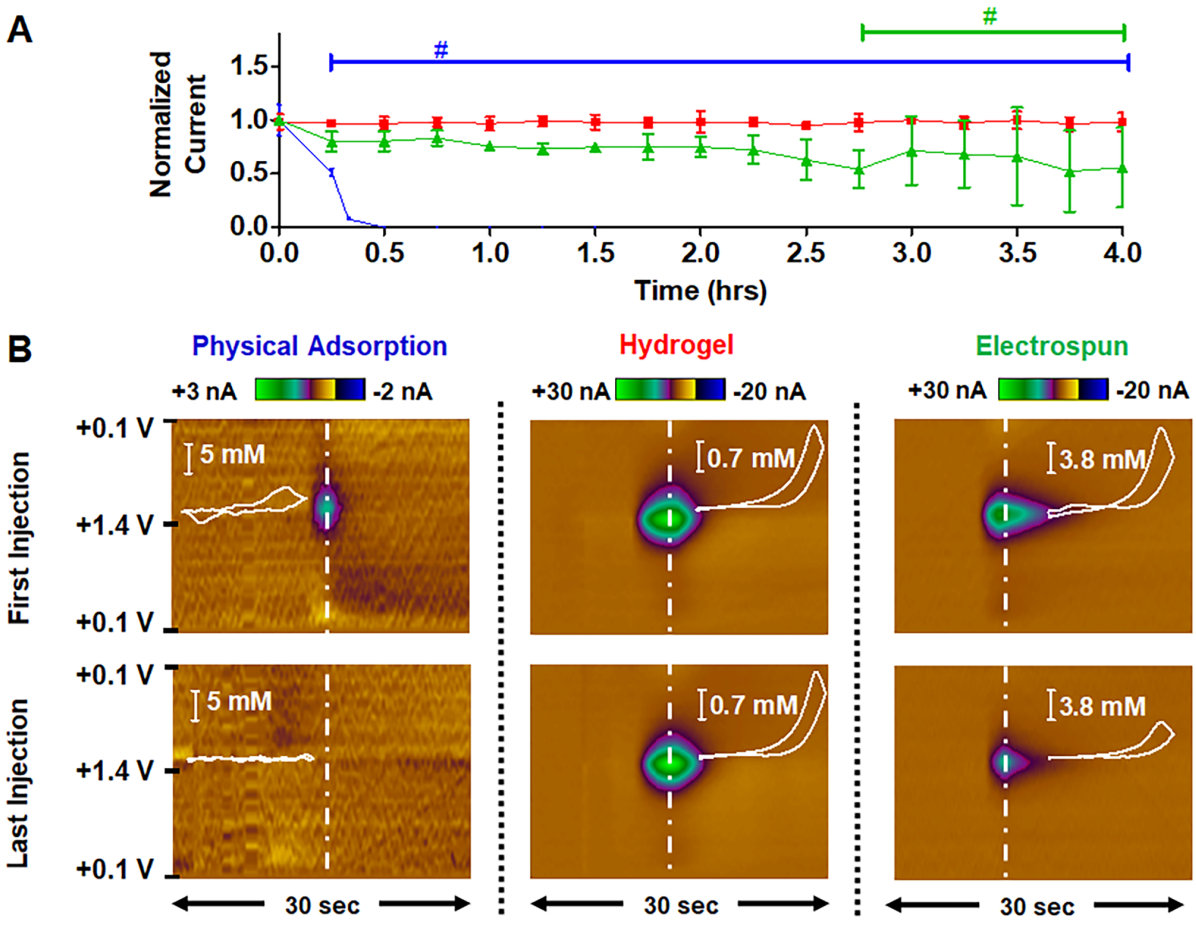

Figure 5. Quantitative assessment of stability. (A) Normalized current collected in repeated glucose measurements (5 mM for physical adsorption, 1.6 mM for entrapment in the chitosan hydrogel or electrospun nanofibers). # denotes significant differences compared to the first injection (two-way ANOVA with Bonferroni posttest, $p<0.05$ – $p<0.001$) (B) Representative color plots depicting data collected in the first (top) vs last (bottom) injection. Insets are voltammograms extracted from the data at the time marked by the dashed white line.

Glucose measurements in live brain tissue.

Microbiosensors fabricated by entrapping GOx in electrospun PVA nanofibers (Figure 6), or in the chitosan hydrogel (Figure 7), were evaluated for performance in live brain tissue. Biosensors created by physical adsorption of the enzyme onto the carbon surface were not further evaluated, due to instability (Figure 5). Figure 6A presents scanning electron micrographs of an electrospun microbiosensor before (left) and after (right) placement in a rat brain slice containing the striatum (middle) for measurements of glucose dynamics in this *ex vivo* preparation. Placement in tissue did not appear to substantially displace the nanofibers; however, some swelling of the fibers is evident. The swelling of PVA fibers upon placement in an aqueous environment has been documented in previous studies.[46, 47] Delivery of a single electrical pulse (450 μA) to the tissue elicited a measurable glucose signal, as well as dopamine release from local terminals in the striatum (Figure 6B). The color plot (left) depicts representative voltammetric data. Molecular dynamics are evident in the concentration vs time plot (right). These data demonstrate a dopamine release event (asterisk in color plot, blue trace) that coincides with the onset of a biphasic increase in extracellular glucose (triangle in color plot, red trace) that endures over at least 8 sec. Glucose delivery to the vicinity of the biosensor is not likely to be due to cerebral blood flow, due the nature of the brain slice preparation. However, astrocytes present in the brain slice contain glycogen and glucose transporter 1, providing a means by which glucose can be delivered to the extracellular space in response to an increase in metabolic demand.[48, 49] However, it is important to note that the amount of glucose monitored immediately after stimulation (~ 0.6 - 1 mM) is close to the

theoretical limit of detection (LOD) for these microbiosensors (Figure 4).

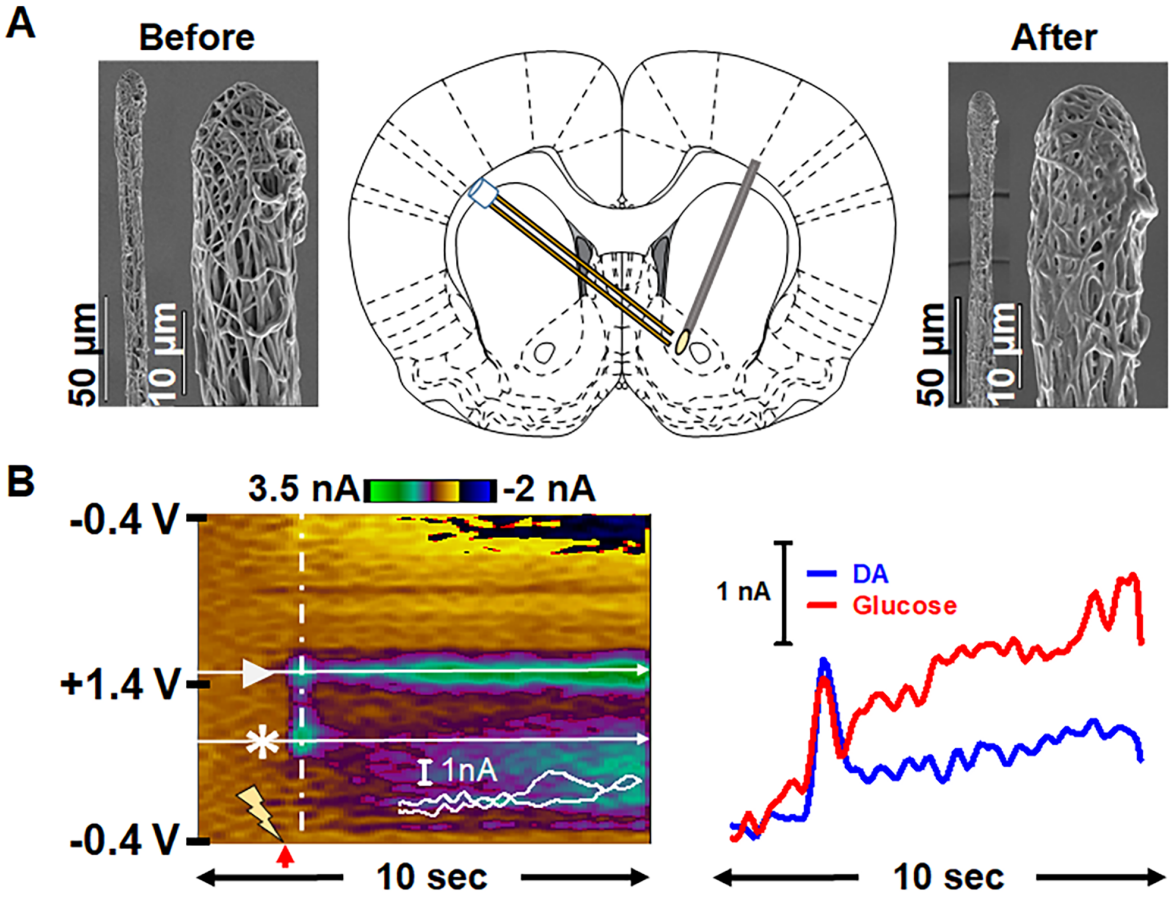

Figure 6. Glucose measurements in a rat brain slice using an electrospun microbiosensor. (a) Scanning electron micrographs depicting the sensor surface before (left) and after (right) tissue implantation. The rat brain slice preparation is depicted in the middle panel. (b) Color plot of voltammetric data collected before and after delivery of a single electrical pulse (450 µA, red arrow). A voltammogram extracted at the time of the white vertical line is inset. Molecular concentration vs time profiles (right) extracted from these data (at the potentials indicated by the horizontal lines) provide dynamic information for both glucose and DA in the vicinity of the biosensor.

In a separate experiment, a microbiosensor fabricated by immobilizing GOx in a chitosan hydrogel was positioned in the dorsal striatum of an anesthetized, intact, male rat (experimental design depicted in Figure 7A). An intravenous infusion of saline (0.6 mL) was followed by electrical stimulation of midbrain neurons in the ventral tegmental area/ substantia nigra region (lightning bolt with red arrow; 60 Hz, 120 pluses, 200 μA), and voltammetric data were recorded at the microbiosensor in the striatum. A representative color plot is presented in Figure 7B, left. Concentration vs time traces extracted from these data (white horizontal lines) reveal an increase in striatal glucose availability (triangle) immediately following dopamine release (asterisk), consistent with previously published results.[9] A voltammogram that serves to identify the analytes was extracted from the data at the time of the white, vertical dashed line (inset). The extracted concentration vs time traces are shown in the panel to the right. We speculate that dopamine release activated local cells in the striatum,[17] increasing metabolic demand. This was accommodated by glucose influx to the region by some combination of an increase in cerebral blood flow and the release of glucose from glycogen reserves within astrocytes.[48, 50] A second (identical) electrical stimulation was delivered 15 min later, immediately following intravenous glucose administration (2.8 mM, Figure 7c). Again, the chitosan hydrogel microbiosensor afforded robust and reliable glucose monitoring. A larger increase in glucose concentration was evoked by this stimulation, suggesting that glucose availability was enhanced by intravenous administration of glucose. Importantly, the data clearly demonstrate that enzyme immobilization by entrapment in a chitosan hydrogel is an

effective method for biosensor fabrication, enabling measurements of brain glucose.

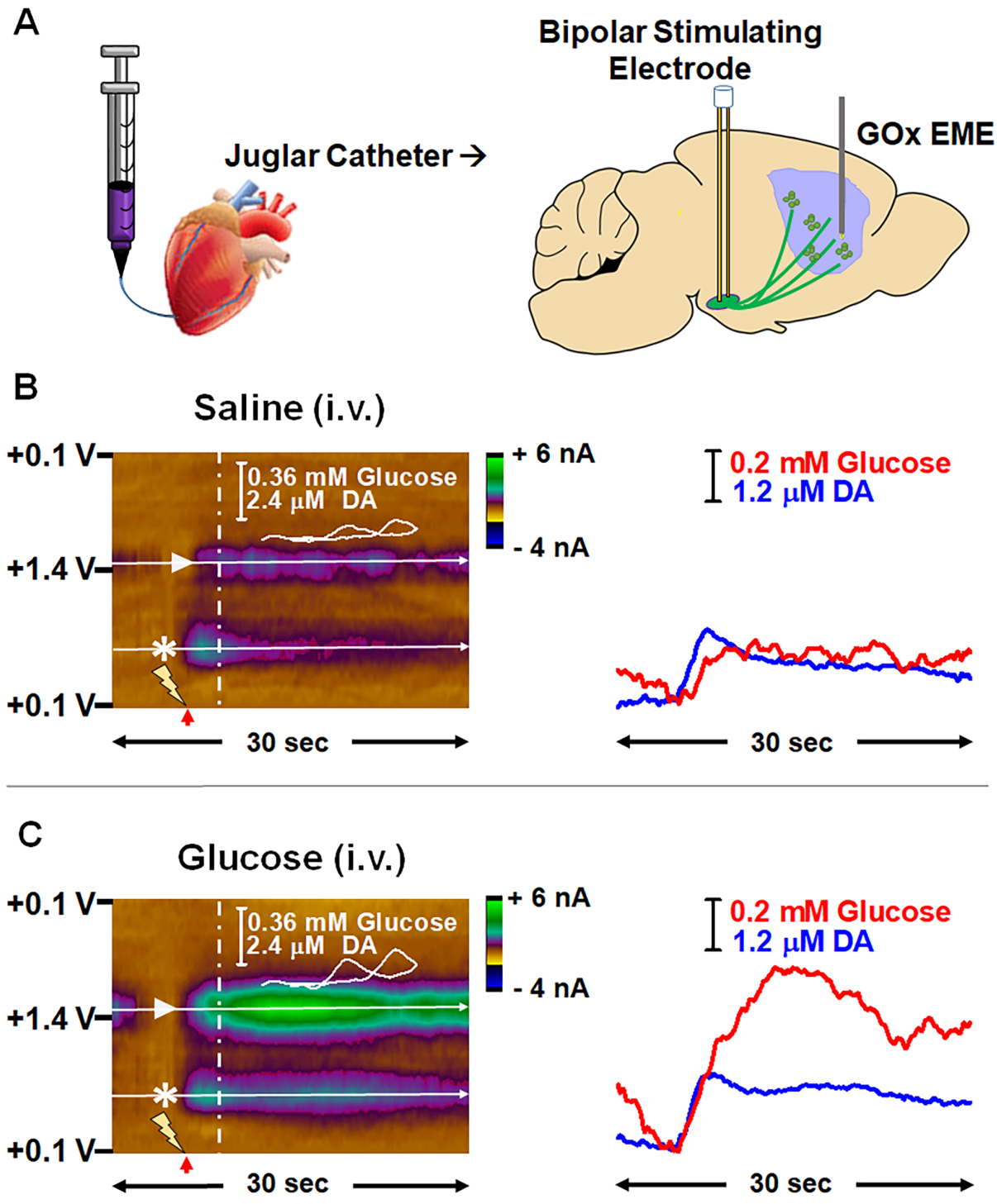

Figure 7. Glucose measurements collected in intact rat striatum using a chitosan hydrogel microbiosensor. A bolus of saline (B) or glucose (C) was administered intravenously.

10.1002/cphc.201701235

Extracellular glucose availability was monitored in response to electrical stimulation (60 Hz, 120 pluses, 200 μA, red arrow) of midbrain neurons projecting to the striatum. Triangle and asterisk indicate the voltammetric signal for glucose and dopamine, respectively. Voltammograms extracted from the data at the time of the vertical dashed line are provided in the inset. Molecular dynamics are plotted in the panels on the right.

Conclusion

This work quantitatively characterizes and compares three strategies of enzyme immobilization at the surface of a carbon-fiber microelectrode. Immobilization of GOx by physical adsorption generates a biosensor with poor sensitivity to glucose (Figure 4), and unstable performance (Figure 5). This is likely due to weak interactions between the enzyme and carbon surface. Thus, this approach is not suitable for extended glucose measurements. Entrapment of GOx in PVA nanofibers electrospun onto a carbon-fiber surface generates microbiosensors that are effective for glucose measurements over a large linear range (Figure 4), and these sensors exhibit stable performance over several hours (Figure 5). This approach may be particularly useful for measurements targeting glucose concentrations in excess of 3 mM, such as in the blood. Finally, entrapment of GOx in the chitosan hydrogel generates microbiosensors capable of sensitive glucose measurements over a 4 h period (Figure 4-5). Both the electrospun and chitosan hydrogel microbiosensors were capable of monitoring robust glucose signals in rat striatal tissue (Figure 6-7). However, the hydrogel immobilization strategy out-performed the other enzyme immobilization strategies, in terms of sensitivity and stability, for glucose measurements at physiologically relevant concentrations.

Experimental

Chemicals. All chemicals were purchased from Sigma-Aldrich (St. Louis, MO) and used as received, unless otherwise noted. *In vitro* electrochemical experiments were conducted in phosphate buffered saline solution (0.1 M PBS, containing 0.138 M NaCl and 0.0027 M KCl) at pH 7.4. Chitosan, β-D-Glucose, and GOx from *Aspergillus niger* were obtained from VWR

International (West Chester, PA). The chitosan was created from shrimp shells and had an approximate molecular weight of 190 –375 kDa with a deacetylation percentage of ≥75% (practical grade). Glucose stock solution was prepared and underwent mutarotation for 24 h at room temperature. All aqueous solutions were made using doubly distilled water >18 MΩ·cm (Millipore Milli-Q, Billerica, MA).

Microelectrode fabrication. Glass-insulated carbon-fiber microelectrodes were fabricated as described previously.[8, 24] Briefly, a single T-650 carbon fiber (7 μm diameter, Cytec Industries, West Patterson, NJ) was aspirated into a borosilicate glass capillary (0.6 × 0.4 mm or 1.0 × 0.5 mm, A-M Systems, Carlsburg, WA) and pulled using a micropipet puller (Narishige, Tokyo, Japan) to create two sealed microelectrodes. The exposed fiber was manually cut under a microscope to a desired length (~100 μm). An electrical connection was established by inserting a stainless steel wire (Squires Electronics, Inc., Cornelius, OR) coated with conductive silver paint (GC Electronics, Rockford, IL) into the back of the microelectrode. Prior to deposition, carbon-fiber microelectrodes were electrochemically conditioned with a voltammetric waveform of −0.4 to +1.4 V at a scan rate of 400 $V \cdot sec^{-1}$ for 15 min at 60 Hz, and then for 5 min at 10 Hz.

Physical adsorption. Conditioned microelectrodes were submerged in an aqueous GOx solution (20 $mg \cdot mL^{-1}$ GOx) for 72 h at 4°C. After a 15 min drying period at room temperature, GOx enzyme-modified electrodes were dip coated in a Nafion solution (D2020, Ion Power, DE) for 10 sec and allowed to dry for 30 sec. The Nafion dip coating process was repeated 3 times. The electrodes were stored at $4^{o}C$ for 24 h prior to testing.

Hydrogel entrapment. Conditioned electrodes were submerged in an aqueous solution containing 20 mg·mL^{-1} GOx (specific activity: 100 U·mg^{-1} at 37 °C) in 2% chitosan (pH ~ 5.3), as previously described.[8, 9] A potential of −3.0 V was applied for ~30 s using a DC power supply to electrodeposit a chitosan hydrogel encapsulating GOx at the electrode surface. GOx-enzyme-modified electrodes were stored in PBS at 4 °C prior to use.

Electrospinning. The electrospinning protocol was adapted from a previously published report.[43] Briefly, an aqueous 9.5 wt% PVA solution was prepared (Mowiol 40-88, average molecular weight 205 kg·mol^{-1}, 88% hydrloized) with 1X TRIS buffer and stored in the fridge 24 h prior to use. The PVA solution was combined with GOx (20 mg·mL^{-1}). The final PVA concentration in the blend was 7 wt.% loaded into a 10 mL syringe fitted with a stainless steel needle. A point-plate configuration was utilized to create the nanofibers with a flow rate of 0.5 mL·hr^{-1}, a 17.5 kV potential (Gamma High Voltage Research, D-ES-30PN/M692) and a collection distance of 15 cm between the tip of the needle and the ground collector plate. An electrochemically conditioned carbon-fiber microelectrode was placed in the line of nanofiber formation and manually rotated at 0.1 rotations per sec for 30 sec. The GOx/PVA nanofibers were chemically crosslinked by glutaraldehyde vapor. Electrodes were positioned for 15 min in a 100 mL container that held 11 mL of glutaraldehyde solution (50% wt) and 200 µL of 12.5 M hydrochloric acid,[43] then allowed to dry at room temperature for 15 min before they were stored at 4^{o}C.

Electrochemical data acquisition. All *in vitro* electrochemical data were collected in a custom flow-injection apparatus at room temperature. Microbiosensors were positioned in a custom electrochemical cell using a micromanipulator (World Precision Instruments, Inc.,

Sarasota, FL), and supplied with a continuous flow of filtered PBS (0.5 mL·min^{-1}) using a syringe pump (New Era Pump Systems, Inc., Wantagh, NY). 2-sec bolus injections of analyte were introduced to the GOx microelectrode surface with a 6-port HPLC valve and pneumonic actuator (Valco Instruments Co., Inc., Houston, TX). The flow-injection apparatus was housed within a custom-built grounded Faraday cage.

Unless otherwise noted, a triangular voltammetric waveform ranging from + 0.1 V to + 1.4 V (vs Ag/AgCl) was applied at 400 V·s^{-1} at a collection rate of 10 Hz using a using a custom instrument (Universal Electrochemistry Instrument, University of North Carolina at Chapel Hill, Department of Chemistry, Electronics Facility). Each potential cycle had a duration of 6.5 ms, and the microelectrode was held at + 0.1 V between scans (Figure 2 A). TH-1 software (ESA, Chelmsford, MA) or HDCV software (University of North Carolina at Chapel Hill, Department of Chemistry, Electronics Facility) was used for waveform output with a DAC/ADC card (NI 6251 M). A second card (NI 6711) was used for triggering the DACs and ADCs and for synchronization of the electrochemical experiment with flow injection. Analog filtering was performed using a 4-pole Bessel filter, 2.5 KHz. Signal processing (background subtraction, signal averaging, and digital filtering) were software controlled.

Brain slice experiment. All animal procedures followed the North Carolina State University & Institutional Animal Care and Use Committee (IACUC) guidelines. Male Sprague-Dawley rats (290 - 320 g, Charles River Laboratories, Raleigh, NC; n = 2) were deeply anesthetized with urethane (1.5 g·kg^{-1}, i.p.). Upon heavy sedation, the rats were decapitated and the brain was rapidly removed, mounted, and placed in cold artificial cerebral spinal fluid (aCSF). Utilizing a vibratome (World Precision Instruments, Sarasota, FL), 400 µm-thick coronal

slices containing the striatum were obtained and allowed to rest in buffer for at least 1 h. Brain slices were placed in a heated recording chamber (Warner Instruments, Hamden, CT) housed in a Faraday cage, and perfused with aCSF buffer maintained at 34 °C for at least 1 hour. Microbiosensor and stimulating electrodes were positioned about 100 µm below the surface of the slice with the aid of a microscope (Nikon Instruments, Inc., Melville, NY). To enable detection of dopamine and glucose in this preparation, data was collected using an 'extended' triangular waveform optimized for dopamine (-0.4 V - 1.4 V, 400 $V \cdot s^{-1}$), applied at 10 Hz. Electrical stimulation of nerve terminals consisted of a single 450 µA biphasic pulse.

***In vivo* experiment.** Male Sprague-Dawley rats (290 - 320 g, Charles River Laboratories, Raleigh, NC; n =1) were anesthetized with urethane (1.5 $g \cdot mL^{-1}$, i.p.) and body temperature was maintained at 37 °C with a heating pad. The animal was placed in a stereotaxic frame (David Kopf Instruments, Tujunga, CA) and a chitosan hydrogel microbiosensor was placed in the caudate putamen (CPu, + 1.2 mm AP, 1.5 mm ML, and – 5.0 to – 7.5 mm DV, relative to bregma). A Ag/AgCl reference electrode was inserted in the contralateral forebrain. A bipolar stimulating electrode was placed in the area of the substantia nigra / ventral tegmental area in the midbrain (–5.8 mm AP, 1.0 mm ML, and – 8.1 mm DV, relative to bregma). Infusion volume was 0.6 mL, manually injected. Data were collected with the triangular waveform (0.1V – 1.4V, 400·s^{-1}) applied at 10 Hz, before and after electrical stimulation consisting of 120 pulses (200 µA) applied at 60 Hz, using a pulse width of 2 ms.

Data Analysis and Statistics. HDCV Analysis software (University of North Carolina at Chapel Hill, Department of Chemistry, Electronics Facility) was used for most aspects of data analysis. The limit of detection (LOD) is defined as three times the standard deviation of the

noise. All data are shown as the mean ± standard error of the mean (SEM). Statistical and graphical analyses were performed using GraphPad Prism 5 (GraphPad Software, Inc., La Jolla, CA). As appropriate, One-Way Analysis of Variance (ANOVA) was used to determine statistical differences. Significance was designated at 0.05.

Acknowledgements

We would like to acknowledge Matt Dausch, Vincent Toups, and Tooba Rashid for voltammetric data collection and analysis. We would also like to thank Barbara Vasconcelos de Farias for assistance with electrospinning, and Chuck Mooney (NCSU Analytical Instrumentation Facility) for acquisition of the SEMs. Funding was provided by the National Science Foundation (CAREER CHE 1151264 to L.A.S.), the Department of Chemistry at North Carolina State University, and the NC State University W.M. Keck Center for Behavioral Biology.

TOC Figure:

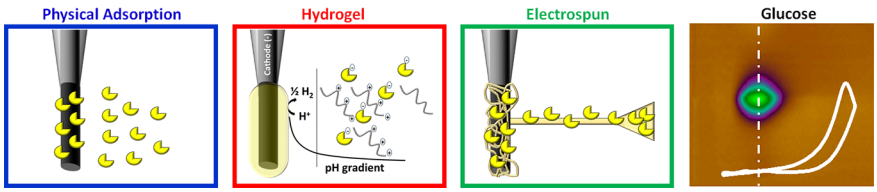

TOC Entry: Glucose oxidase-modified carbon-fiber microelectrodes can be combined with fast-scan cyclic voltammetry for real-time measurements of glucose fluctuations in brain tissue. Work presented herein quantitatively compares three approaches to enzyme immobilization on the microelectrode surface - physical adsorption, hydrogel entrapment, and entrapment in electrospun nanofibers. The data suggest that each of these methods can be used to create

10.1002/cphc.201701235

functional microbiosensors, but hydrogel entrapment is the most effective in terms of sensitivity and stability.

References:

[1] L. C. Clark, C. Lyons, *Ann. N. Y. Acad. Sci.* **1962**, *102*, 29-45.
[2] A. Sassolas, L. J. Blum, B. D. Leca-Bouvier, *Biotechnol Adv* **2012**, *30*, 489-511.
[3] K. N. Hascup, E. R. Hascup, M. L. Stephens, P. E. Glaser, T. Yoshitake, A. A. Mathe, G. A. Gerhardt, J. Kehr, *Neuropsychopharmacology* **2011**, *36*, 1769-1777.
[4] K. M. Wassum, V. M. Tolosa, T. C. Tseng, B. W. Balleine, H. G. Monbouquette, N. T. Maidment, *J Neurosci* **2012**, *32*, 2734-2746.
[5] V. Parikh, R. Kozak, V. Martinez, M. Sarter, *Neuron* **2007**, *56*, 141-154.
[6] W. M. Howe, H. J. Gritton, N. A. Lusk, E. A. Roberts, V. L. Hetrick, J. D. Berke, M. Sarter, *J. Neurosci.* **2017**, *37*, 3215-3230.
[7] V. P. Zanini, B. López de Mishima, V. Solís, *Sens. Actuators, B* **2011**, *155*, 75-80.
[8] L. Z. Lugo-Morales, P. L. Loziuk, A. K. Corder, J. V. Toups, J. G. Roberts, K. A. McCaffrey, L. A. Sombers, *Anal. Chem.* **2013**, *85*, 8780-8786.
[9] S. K. Smith, C. A. Lee, M. E. Dausch, B. M. Horman, H. B. Patisaul, G. S. McCarty, L. A. Sombers, *ACS Chem Neurosci* **2017**, *8*, 272-280.
[10] X. H. Chen, N. Matsumoto, Y. B. Hu, G. S. Wilson, *Anal. Chem.* **2002**, *74*, 368-372.
[11] G. S. Wilson, R. Gifford, *Biosens. Bioelectron.* **2005**, *20*, 2388-2403.
[12] U. Hanefeld, L. Gardossi, E. Magner, *Chem. Soc. Rev.* **2009**, *38*, 453-468.
[13] Z.-G. Wang, L.-S. Wan, Z.-M. Liu, X.-J. Huang, Z.-K. Xu, *J. Mol. Catal. B: Enzym.* **2009**, *56*, 189-195.
[14] G. S. Wilson, R. Gifford, *Biosens. Bioelectron.* **2005**, *20*, 2388-2403.
[15] R. Asri, B. O'Neill, J. C. Patel, K. A. Siletti, M. E. Rice, *Analyst* **2016**, *141*, 6416-6421.
[16] M. E. Fox, M. A. Mikhailova, C. E. Bass, P. Takmakov, R. R. Gainetdinov, E. A. Budygin, R. M. Wightman, *Proc. Natl. Acad. Sci. U. S. A.* **2016**, *113*, 6985-6990.
[17] C. Owesson-White, A. M. Belle, N. R. Herr, J. L. Peele, P. Gowrishankar, R. M. Carelli, R. M. Wightman, *J. Neurosci.* **2016**, *36*, 6011-6021.
[18] M. W. Howe, P. L. Tierney, S. G. Sandberg, P. E. Phillips, A. M. Graybiel, *Nature* **2013**, *500*, 575-579.
[19] J. J. Day, M. F. Roitman, R. M. Wightman, R. M. Carelli, *Nat. Neurosci.* **2007**, *10*, 1020-1028.
[20] R. M. Wightman, C. Amatore, R. C. Engstrom, P. D. Hale, E. W. Kristensen, W. G. Kuhr, L. J. May, *Neuroscience* **1988**, *25*, 513-523.
[21] K. T. Kishida, I. Saez, T. Lohrenz, M. R. Witcher, A. W. Laxton, S. B. Tatter, J. P. White, T. L. Ellis, P. E. Phillips, P. R. Montague, *Proc. Natl. Acad. Sci. U. S. A.* **2016**, *113*, 200-205.
[22] R. M. Wightman, *Science* **2006**, *311*, 1570-1574.
[23] M. L. Huffman, B. J. Venton, *Analyst* **2009**, *134*, 18-24.
[24] J. G. Roberts, L. Z. Lugo-Morales, P. L. Loziuk, L. A. Sombers, *Methods Mol. Biol.* **2013**, *964*, 275-294.
[25] R. L. McCreery, *Chem. Rev.* **2008**, *108*, 2646-2687.

[26] J. Roberts, L. Lugo-Morales, P. Loziuk, L. Sombers, in *Dopamine, Vol. 964* (Ed.: N. Kabbani), Humana Press, **2013**, pp. 275-294.
[27] J. G. Roberts, B. P. Moody, G. S. McCarty, L. A. Sombers, *Langmuir* **2010**, *26*, 9116-9122.
[28] E. C. Mitchell, L. E. Dunaway, G. S. McCarty, L. A. Sombers, *Langmuir* **2017**, *33*, 7838-7846.
[29] S. Hafizi, Z. L. Kruk, J. A. Stamford, *J. Neurosci. Methods* **1990**, *33*, 41-49.
[30] A. L. Sanford, S. W. Morton, K. L. Whitehouse, H. M. Oara, L. Z. Lugo-Morales, J. G. Roberts, L. A. Sombers, *Anal. Chem.* **2010**, *82*, 5205-5210.
[31] C. Bonnet, S. Andreescu, J.-L. Marty, *Anal. Chim. Acta* **2003**, *481*, 209-211.
[32] E. M. I. M. Ekanayake, D. M. G. Preethichandra, K. Kaneto, *Biosensors and Bioelectronics* **2007**, *23*, 107-113.
[33] T. F. Tseng, Y. L. Yang, M. C. Chuang, S. L. Lou, M. Galik, G. U. Flechsig, J. Wang, *Electrochem commun* **2009**, *11*, 1819-1822.
[34] E. N. Navera, M. Suzuki, E. Tamiya, T. Takeuchi, I. Karube, *Electroanalysis* **1993**, *5*, 17-22.
[35] B. Krajewska, *Enzyme Microb. Technol.* **2004**, *35*, 126-139.
[36] H. Yi, L.-Q. Wu, W. E. Bentley, R. Ghodssi, G. W. Rubloff, J. N. Culver, G. F. Payne, *Biomacromolecules* **2005**, *6*, 2881-2894.
[37] A. Greiner, J. H. Wendorff, *Angew. Chem. Int. Ed.* **2007**, *46*, 5670-5703.
[38] M. Scampicchio, A. Arecchi, N. S. Lawrence, S. Mannino, *Sens. Actuators, B* **2010**, *145*, 394-397.
[39] C. Tang, C. D. Saquing, J. R. Harding, S. A. Khan, *Macromolecules* **2010**, *43*, 630-637.
[40] J. H. Lee, U. S. Lee, K. U. Jeong, Y. A. Seo, S. J. Park, H. Y. Kim, *Polym. Int.* **2010**, *59*, 1683-1689.
[41] D. Li, Y. N. Xia, *Advanced Materials* **2004**, *16*, 1151-1170.
[42] G. Ren, X. Xu, Q. Liu, J. Cheng, X. Yuan, L. Wu, Y. Wan, *React. Funct. Polym.* **2006**, *66*, 1559-1564.
[43] C. Tang, C. D. Saquing, S. W. Morton, B. N. Glatz, R. M. Kelly, S. A. Khan, *ACS Appl Mater Interfaces* **2014**, *6*, 11899-11906.
[44] J. P. Lowry, R. D. O'Neill, M. G. Boutelle, M. Fillenz, *J Neurochem* **1998**, *70*, 391-396.
[45] C. Chen, Q. J. Xie, D. W. Yang, H. L. Xiao, Y. C. Fu, Y. M. Tan, S. Z. Yao, *Rsc Advances* **2013**, *3*, 4473-4491.
[46] S. D. Zhang, Y. C. Zhai, Z. F. Zhang, *Appl Mech Mater* **2011**, *84-85*, 485.
[47] X. Tong, J. Zheng, Y. Lu, Z. Zhang, H. Cheng, *Mater. Lett.* **2007**, *61*, 1704-1706.
[48] O. B. Paulson, S. G. Hasselbalch, E. Rostrup, G. M. Knudsen, D. Pelligrino, *J Cereb Blood Flow Metab* **2009**, *30*, 2-14.
[49] F. Binkofski, M. Loebig, K. Jauch-Chara, S. Bergmann, U. H. Melchert, H. G. Scholand-Engler, U. Schweiger, L. Pellerin, K. M. Oltmanns, *Biol. Psychiatry* **2011**, *70*, 690-695.
[50] P. Mergenthaler, U. Lindauer, G. A. Dienel, A. Meisel, *Trends Neurosci* **2013**, *36*, 587-597.